

In-situ Self-calibration of Terrestrial Laser Scanners and Deformation Analysis Using Both Signalized Targets and Intersection of Planes for Indoor Applications

Jacky C.K. CHOW, William F. TESKEY, and J.W. (Bill) LOVSE, Canada

Key words: Terrestrial laser scanning, calibration, deformation monitoring, geometric modeling, point cloud

SUMMARY

Terrestrial laser scanners are high-accuracy 3D imaging instruments that are capable of measuring deformations with sub-millimetre level accuracy in most close-range applications. Traditionally, deformation monitoring is performed using distinct signalized targets. In this case, the centroids of these targets must be determined with great accuracy. A least-squares based target centroid extraction algorithm for planar checkerboard/chessboard targets is proposed for laser scanner data. These targets are used in a free-station network for performing deformation analysis with no assumptions about the deformation pattern. To ensure the optimum measurement accuracy of the instrument, all systematic errors inherent to the instrument at the time of data acquisition need to be removed. One method for reducing these systematic errors is self-calibration of terrestrial laser scanners. In this paper, this was performed on-site to model the systematic errors in the raw observations of the scanner. Post self-calibration, the accuracy of the measured translation movements were improved from the millimetre level to the sub-millimetre level.

Despite the outstanding performance of using laser scanners with signalized targets in deformation analysis, the main benefit of active sensors like terrestrial laser scanning systems is its ability to capture 3D information of the entire scene without markers. A new markerless deformation analysis technique that utilizes intersection points derived from planar-features is proposed and tested in this paper. The extraction and intersection of planes in each point cloud can be performed automatically or semi-automatically. This new method is based on free-stationing and does not require a priori knowledge about stable control points. It can detect and measure translational and rotational movements of the planes with minimal human interaction. This paper will present both simulated and real results, demonstrating the performance of the newly proposed methodology.

In-situ Self-calibration of Terrestrial Laser Scanners and Deformation Analysis Using Both Signalized Targets and Intersection of Planes for Indoor Applications

Jacky C.K. CHOW, William F. TESKEY, and J.W. (Bill) LOVSE, Canada

1. INTRODUCTION

Deformation analysis is a common task in surveying and structural engineering. Typically this can be done noninvasively using total stations, photogrammetry, or laser scanners. For outdoor applications, terrestrial laser scanning (TLS) has been used in land/rock deformation monitoring (Monserrat & Crosetto, 2007; Alba & Scaioni, 2010). For indoor TLS applications, the deflection of structural beams has been measured with sub-millimetre level accuracy (Gordon & Lichti, 2007; Rönnholm et al., 2009). The performance of modern static terrestrial laser scanners for detecting and measuring deformations in an indoor environment is explored in this paper. The well-established point-based deformation analysis method forms the basis of this paper. Although the accuracy of a single point in a laser scanner point cloud is inferior when compared to high-precision total stations, by exploiting the large redundancy, unique targets can be extracted from the point cloud with great accuracy. These targets can either be signalized targets with a radiometric pattern, or they can be derived from geometric features such as the intersection of three planes. From simulation and real data, it is evident that translational movements can be reliably identified and measured automatically with accuracy in the sub-millimetre level. To ensure this level of accuracy, it is crucial that all blunders and systematic errors are removed from the data. Systematic errors can usually be reduced if not eliminated when in both epochs the same sensor is used to capture data with similar network geometry, and over a short period of time. Alternatively, this paper shows that the laser scanner self-calibration is an effective tool for modelling the sensor errors. The accuracy of the recovered deformations improved from a few millimetres to the sub-millimetre level after self-calibration. By adopting the intersection of planar surfaces as targets, after the point-based deformation analysis the rotational movements of the planes can be measured as well. This can give a better description of the deformation pattern in the scene than the conventional method.

2. METHODOLOGY

2.1 Point-based Deformation Analysis Method

The conventional 3D deformation monitoring technique explained in Gründig et al. (1985) forms the core structure of the newly proposed methodology. This widely adopted method allows the 3D translations of common targets observed in two epochs to be detected and

measured. The fundamental procedure is summarized here for completeness. First, a network adjustment is performed separately for both epochs. The datum is defined using inner-constraints with all the targets in the object space included. Systematic errors should be reduced if not eliminated. All outliers are identified and removed from the network, for example through Baarda's data snooping. Since the raw observations of a TLS instrument are range (ρ), horizontal direction (θ), and vertical angle (α), the network adjustment should be performed in the spherical coordinate system instead of the Cartesian coordinate system. Variance component estimation should be performed to ensure proper weighting of the observations. After each individual epoch has been properly adjusted, a series of statistical tests such as Bartlett's Test and the Global Congruency Test can be carried out. Every target point should be tested for movement after the contribution of each point to the network has been isolated. The target point with the most significant movement is eliminated from the datum using the S-transformation. This point localization/isolation and elimination repeats until no statistically significant movements among the target points are detected. The effectiveness of this deformation analysis method depends greatly on the target measurement accuracy. In the next section, a least-squares approach for deriving the centroid of a checkerboard type target in a laser scanner point cloud is explained.

2.1.1 Checkerboard/chessboard Target Centroid Extraction Algorithm

The centroid of a checkerboard target (Figure 1a) can be measured semi-automatically in a similar fashion as measuring the centroid of circular planar targets (Chow et al., 2010a). A seed point is manually selected near the centroid of the target. The target can then be segmented from the point cloud based on a fixed radial distance (Figure 1b). Since the target is planar, the parameters of the best-fit plane can be computed using either least-squares adjustment or orthogonal regression (Shakarji, 1998) and the point cloud can be rotated into the plane's coordinate system. The irregular structure of a laser scanner point cloud makes it difficult to identify sharp transitions in radiometric properties, so the point cloud is resampled using bilinear interpolation. The edges of the checkerboard in the gridded intensity image can then be extracted with ease using a high-pass filter, such as the Canny edge detector (Figure 1c). The two edges (crosshairs) of the target can be separated using RANSAC line fitting and the planimetric centroid of the signaled target is defined as the intersection of the two lines with a least-squares constraint maintaining the orthogonality of the lines. The orthogonal distance to the best-fit plane gives the third dimension of the centroid. Finally, after reversing the rotations, the 3D coordinates of the checkerboard target in the scanner space are obtained (Figure 1d). This method works well regardless of the checkerboard target orientation and with low density point clouds as well. The accuracy of the extracted centroids using this method is similar to measurements made with the Leica Cyclone software. Major benefits of this method compared to Cyclone are efficiency, reduced human interaction, and full variance-covariance information for every target.

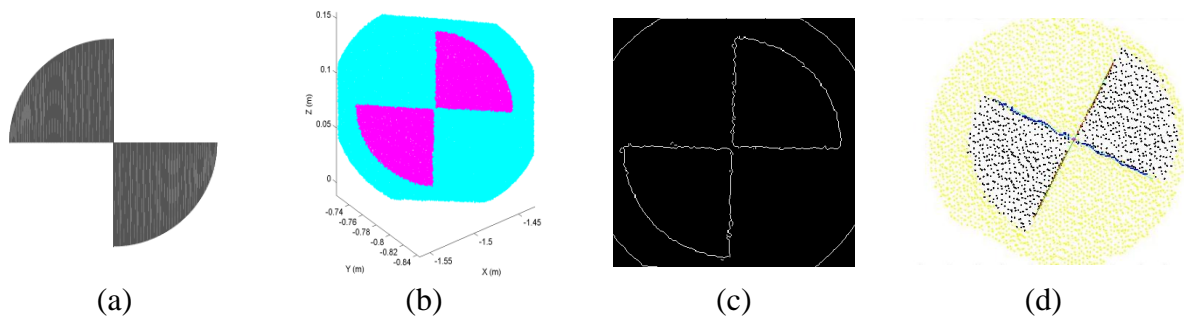


Figure 1: a) Digital image of the checkerboard target design. b) Point cloud of the signalized target after segmentation with the colour difference indicating the difference in intensity. c) Binary image of the target after performing Canny edge detector to the gridded intensity image. d) The centroid of the target measured as the intersection of two orthogonal lines.

2.2 Plane-based Deformation Analysis Method

One of the benefits of active 3D imaging sensors like TLS instruments is their ability to make dense measurements on smooth surfaces without the need of any textures. In urban environments, planar features are encountered frequently. In addition, among the various geometric features, planes are one of the easiest to model mathematically. Deformation analysis using planar features had been proposed previously by Lindenbergh et al. (2005) and Gielsdorf et al. (2008). In this paper, a simpler deformation analysis technique using planes is presented. It is based on a network of intersection points; therefore at each epoch more than one scan needs to be captured with no less than four non-parallel planes. This new method begins by extracting planes with various orientations and distances from the point cloud (e.g. the ceiling, walls, and floor). This can be achieved either through manual segmentation or automatic classification and segmentation of features in the point cloud (Vosselman et al., 2004; and Belton & Lichti, 2006). The best-fit plane parameters for every flat surface are estimated using least-squares adjustment with the observations expressed in the spherical coordinate system. To accommodate for the varying incidence angle of the laser, the standard deviation for the range observations is set to be proportional to the secant of the incidence angle (Soudarissanane et al., 2011). After computing the plane parameters, intersection points can be uniquely determined from the intersection of three planes and used as targets. Given m number of planes, the maximum number of intersection points is ${}_m C_3$. However, if any two of the three planes are nearly parallel, an accurate intersection point is unlikely to be achievable. An intersection point is best determined geometrically when the three planes are mutually orthogonal. Hence, only planes with an intersection angle greater than a threshold value should be utilized for determining the intersection points. These intersection points will serve as targets in each scan, and since there is point-to-point correspondence, the conventional point-based deformation analysis technique explained in Section 2.1 can be directly applied. This approach is more effective than merely using the points of maximum curvature in the point cloud because even virtual corners can be used as targets in the network adjustment, which increases the redundancy.

Although the point-based deformation analysis approach is widely adopted, it has its limitations. One of the drawbacks of the point-based deformation analysis technique is that only 3D translational movements can be estimated for the targets. Compared to total stations, one of the advantages of TLS instruments is that the entire scene is mapped, rather than just individual target points. By using geometric primitives such as planes instead of points, rotational movements can be recovered in addition to the translational movements. After the intersection points with significant deformations are identified, the planes which might have moved can be easily recognized if the composition of each intersection point is known. The plane that composes the majority of deformed intersection points, especially the points with the most statistically significant deformations, is identified and the movement of that plane is calculated. By assuming that all planes behave as rigid bodies, the three rotations and three translations of a particular plane between two epochs can be estimated using the rigid body transformation. The intersection points belonging to the moving plane in both epochs will be the observations. This can be accomplished efficiently without any initial approximations using Horn's Method (Horn, 1987). Although six degrees of freedom can be calculated, not all of them are physically realized because translations orthogonal to the normal axis and rotations about the normal axis of the plane cannot be measured. Alternatively, the rotational and translational movements of a plane can be estimated as the spatial angle between the normal axes of the moving plane and the change in orthogonal distance, respectively. This method of deformation analysis eliminates the need for signalized targets and is a simple modification to the well-established point-based deformation analysis technique. It is based on free-stationing and it can detect and measure deformations in the scene automatically.

3. RESULTS FROM SIMULATION

3.1 Point-based Deformation Simulation

To determine the achievable level of accuracy and precision when using TLS instruments with the conventional point-based deformation analysis technique, a simulation is performed. A 14 m by 11m by 3m rectangular room is designed with 62 targets randomly distributed on the walls, floor, and ceiling (Figure 2). Six scans were captured from two locations, where at each location the scanner has an initial heading that is rotated 120° clockwise from the previous one. The scanner is assumed to have an unrestricted field of view with a range precision of 1mm and an angular measurement precision of 15". These values were chosen based on a recent self-calibration of the Leica HDS6100 scanner. Data from two epochs were simulated with the same scanner design and similar network geometry. In the second epoch, two targets at different distances away from the first scan station (3.5m and 11m) were shifted. For the closer target, a 5cm translation in the x-direction was introduced and for the farther target, 5cm translations in both the y-direction and negative x-direction were introduced. The recovered translations (T_x , T_y , and T_z) along with their standard deviations (σ_{T_x} , σ_{T_y} , and σ_{T_z}) are presented in Table 1. In this simulation, it appears the deformation can be recovered with accuracy and precision better than the millimeter-level.

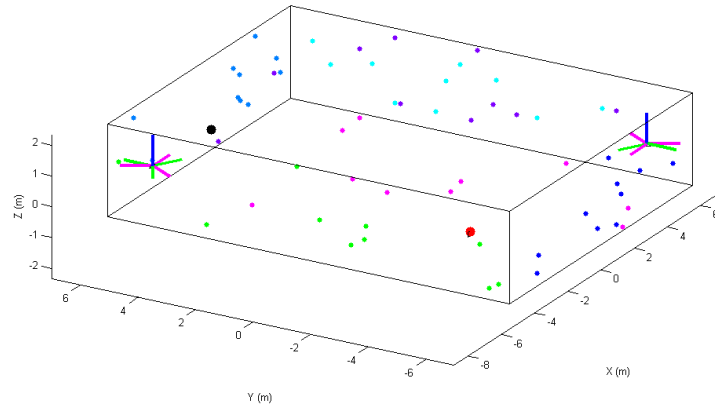


Figure 2: Geometry of simulated room used in the point-based deformation test. The magenta, green, and blue lines indicate the x, y, and z axis of the scan stations, respectively. The black and red dot represent the targets that will be shifted.

Table 1: Recovered translational movement of targets using the point-based deformation analysis method in simulation

| Target Dist (m) | T_x (cm) | T_y (cm) | T_z (cm) | σ_{Tx} (cm) | σ_{Ty} (cm) | σ_{Tz} (cm) |
|-----------------|------------|------------|------------|--------------------|--------------------|--------------------|
| 3.5 | 5.01 | 0.02 | -0.01 | 0.06 | 0.02 | 0.02 |
| 11.0 | -4.93 | 4.95 | -0.05 | 0.05 | 0.05 | 0.04 |

3.2 Plane-based Deformation Simulation

In the plane-based deformation scenario, a room with similar dimensions as before is simulated. There are 8 walls, a ceiling, and a floor arranged to simulate the actual room used in the real experiment (Figure 3). A scanner with the same specifications as before is simulated. Six scans from two locations at the opposite corners of the room were captured, with the assumption that the scanner's field of view was not being obstructed. A 15cm by 15cm plane located either 3.5m north of the first scan station or 8m east of the first scan station was moved in the second epoch. A total of 21 planes were segmented in each epoch, and 200 randomly distributed points are observed on each segmented plane. This point density is low for modern terrestrial laser scanners, and is chosen to demonstrate the achievable performance of the proposed method even with low-density point clouds. Table 2 shows the recoverability of the proposed plane-based deformation method for both translational and rotational movements. The recovered translations are precise and accurate to a level better than sub-millimetre. Rotational movements are measured within precision and accuracy of a few arc minutes.

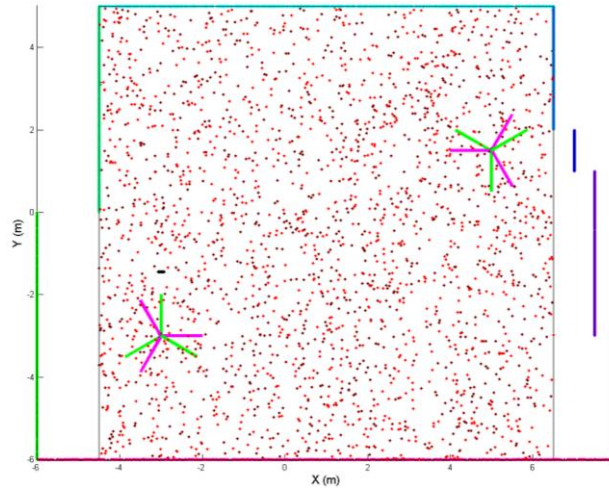


Figure 3: Top view of the simulated room used for testing the plane-based deformation analysis method. The magenta and green lines indicate the x and y axes of a scan station, respectively.

Table 2: Recovered translational and rotational movement of the planes using the newly proposed markerless method in simulation

| Target Dist (m) | True Deformation | | Recovered Deformation | | | |
|--------------------|------------------|-----------|-----------------------|------------------------------|-----------|----------------------------|
| | Shift (cm) | Rotation | Shift (cm) | σ_{shift} (cm) | Rotation | σ_{rotation} |
| 3.5 | 5.000 | 10°00'00" | 5.000 | 0.004 | 10°02'04" | 0°02'46" |
| 8.0 | 5.000 | 10°00'00" | 5.000 | 0.003 | 9°59'21" | 0°02'34" |

4. RESULTS FROM REAL DATA

4.1 Point-based Deformation Results

Three separate datasets were captured in a 14m by 11m by 3m room at the University of Calgary (Figure 4a). Each dataset consisted of signalized targets acquired by the TLS instrument at different positions and orientations. Translational movements were introduced between the two epochs using a bi-directional translation stage (Figure 4b). In the first dataset, six levelled scans were captured using the Leica HDS6100 laser scanner in both epochs. The scanner occupied two locations with varying heading orientations. A total of 62 checkerboard-style signalized targets were fixed to the walls, ceiling, and floor. In the second epoch, the scanner was set up at locations similar to the first epoch. Since the deformation analysis technique being tested is based on free-stationing, the scanner location does not need to be reestablished accurately between the two epochs. In the second dataset, 99 checkerboard targets were scanned using the HDS6100. The two epochs were captured a day apart and on each day four scans were acquired from two different locations. The last dataset consisted of 84 checkerboard targets. Comparable to the second dataset, four levelled scans were captured from two locations in both epochs. However, in this case the first epoch was

captured using the Trimble GS200 laser scanner and after a few hours the second epoch was captured using the HDS6100.



Figure 4: a) Room used for the deformation analysis experiments. b) Signalized target mounted on a translation stage

In the first dataset, two checkerboard targets that were 3.5m and 11m away from the first scan station were translated between the two epochs. The closer target was moved 5cm north and the farther target was moved 5cm north and 5cm west. The normal axes of both planar checkerboard targets were pointing towards the scanner. Table 3 shows the recovered deformations for both targets using the conventional point-based deformation technique. Over a short duration of time and using the same scanner, performing self-calibration of the scanner was deemed unnecessary, even though significant systematic errors were identified. With or without the sensor error modeling the translational movements can be measured with sub-millimetre level accuracy and precision.

Table 3: Recovered translational movement of targets from applying the point-based deformation analysis method to the first dataset

| Target Dist (m) | T_x (cm) | T_y (cm) | T_z (cm) | σ_{Tx} (cm) | σ_{Ty} (cm) | σ_{Tz} (cm) |
|-----------------|------------|------------|------------|--------------------|--------------------|--------------------|
| 3.5 | 5.01 | 0.01 | 0.05 | 0.04 | 0.04 | 0.03 |
| 11 | -4.98 | 5.01 | 0.05 | 0.08 | 0.09 | 0.09 |

The second dataset had two targets that were approximately 4m and 8m away from the first scan station. The farther target faced the scanner, while the closer target was rotated 45° away from the scanner. The introduced and recovered deformations for this dataset are given in Table 4. Similar to the first dataset, the deformations are measured with sub-millimetre level accuracy even without self-calibration.

Table 4: Recovered translational movement of targets from applying the point-based deformation analysis method to the second dataset

| Target Dist (m) | True Translation (cm) | Recovered Translation (cm) |
|-----------------|-----------------------|----------------------------|
| 4 | 5.00 | 5.00 |
| 8 | 5.00 | 5.01 |

The final dataset had two targets set up in similar fashion as the second dataset. Table 5 shows the quality of the point-based deformation analysis method before and after on-site TLS self-calibration. The self-calibration is performed based on the approach explained in Lichti (2007) and following the same notations, the error models for the GS200 and HDS6100 are given in Equations 1 and 2, respectively. The statistically significant systematic errors for the GS200 are the rangefinder offset (a_0) and horizontal encoder circle eccentricity (b_8). The significant systematic errors for the HDS6100 were different from the GS200; they were the laser axis vertical offset (a_2) and the non-orthogonality of encoder circle and vertical axis (b_3 and b_4). The value of each systematic error along with its standard deviation is shown in Table 6.

Table 5: Recovered translational movement of targets from applying the point-based deformation analysis method to the third dataset before and after TLS self-calibration

| Target Dist (m) | True Translation (cm) | Recovered Translation (cm) | |
|-----------------|-----------------------|----------------------------|-------------------|
| | | Before Calibration | After Calibration |
| 4 | 5.00 | 4.75 | 4.99 |
| 8 | 5.00 | 4.55 | 4.94 |

$$\Delta\rho = a_0 \qquad \Delta\theta = b_8 \cos(\theta) \qquad 1$$

$$\Delta\rho = a_2 \sin(\alpha) \qquad \Delta\theta = b_3 \sin(2\theta) + b_4 \cos(2\theta) \qquad 2$$

Table 6: Statistically significant systematic errors for the HDS6100 and GS200

| Coefficient | Value | Standard Deviation |
|-------------|-------|--------------------|
| a_0 [mm] | 2.9 | 0.7 |
| a_2 [mm] | 1.4 | 0.6 |
| b_3 ["] | -8.0 | 4.0 |
| b_4 ["] | -13.4 | 3.7 |
| b_8 ["] | 39.2 | 10.5 |

When the two epochs are captured over a short period of time, the intrinsic parameters of the HDS6100 are relatively stable, and since deformation analysis can be thought of as a simple subtraction process, majority of the unmodelled systematic errors are reduced if not eliminated through subtraction. In Lichti (2007) and Chow et al. (2010b), it has been shown that for some laser scanners, the short-term stability of the systematic errors could be in

question. From the second dataset, it appears that even though there is a slight difference in calibration parameters for the HDS6100 over a 24 hour period, the effect on the point cloud is negligible. However, if different scanners were used to acquire the data, sensor calibration is critical in high accuracy applications even if the data is captured on the same day. From Table 5 it can be seen that the accuracy of deformation measurements can be improved by an order of magnitude after self-calibration. If the same scanner is used for both epochs, but the two epochs are far apart and/or there are reasons to suspect the instability of the sensor's interior orientation parameters, TLS self-calibration should still be performed.

4.2 Plane-based Deformation Results

The same point clouds from datasets 1 and 2 in the point-based deformation experiment above were used for testing the plane-based deformation method. Instead of using signalized targets, 10 planes were extracted from each of the scans (Figure 5a). In the first dataset, a 15cm diameter disk approximately 3.5m away and orthogonal to the first scan station was shifted 5cm away between the two epochs. In the deformation analysis, the disk was identified as the plane experiencing the most significant deformations and the translational movement was measured to be $5.03\text{cm} \pm 0.01\text{cm}$.

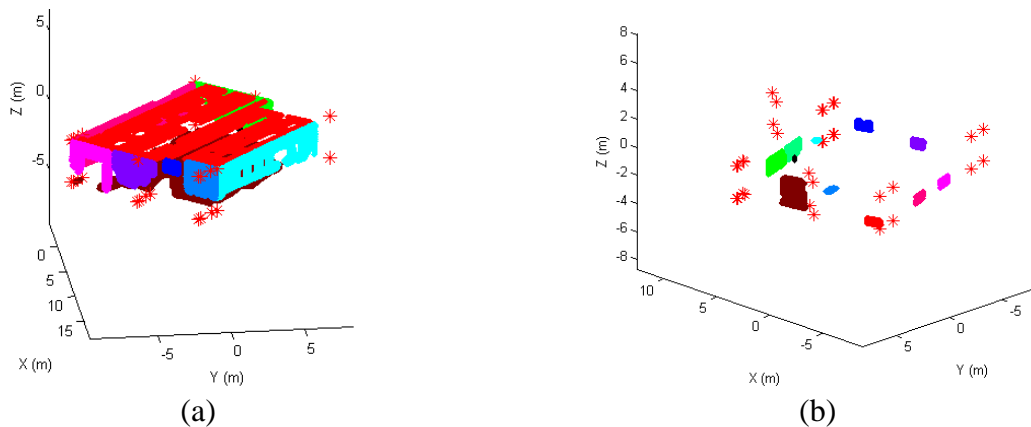


Figure 5: a) Extracted planes from the first dataset. b) Extracted planes from the second dataset for the plane-based deformation analysis

In the second dataset, only the two scans captured near the centre of the room were used in both epochs. The 10 horizontal and vertical planes extracted from the room are smaller than the first dataset, as none exceed 2m in dimensions (Figure 5b). Two disks (15cm in diameter) were placed on a translation stage 4m away from the scan station and shifted 5cm away. One of the disks was orthogonal to the scanner and the other inclined at 45° relative to the scanner. A white 25cm by 25cm square spectralon target was rotated by approximately 30° about its vertical axis using a Manfrotto camera tripod (Figure 6). All deformations were detected automatically and the recovered translational and rotational deformations are shown in Table 7.



Figure 6: Spectralon target mounted on a camera tripod with a tri-axis rotation head

Table 7: Recovered translational and rotational movements of targets from applying the plane-based deformation analysis method to the second dataset

| | True Deformation | Measured Deformation |
|-------------------|------------------|----------------------|
| Orthogonal Target | 5.00cm | 4.96cm |
| Inclined Target | 5.00cm | 4.99cm |
| Rotated Plane | $\sim 30^\circ$ | $30^\circ 15' 08''$ |

The accuracy of the recovered deformations is comparable to the simulation. Translational movements can be recovered with accuracy better than a millimeter. Since the walls, ceiling, and floor are not perfectly flat, restricting the size of the planes improves the accuracy of the deformation measurements. This allows the use of two scans instead of six scans in the network, while maintaining a similar level of accuracy. The accuracy of this approach for measuring rotational movements cannot be adequately assessed at this point because a proper rotational stage was not available, but the results from this preliminary testing appear to agree with the simulation.

5. CONCLUSIONS

The conventional point-based deformation analysis technique has been applied to laser scanning data. After removing the systematic errors and blunders, translational movements can be automatically detected and measured with accuracy better than a millimetre. Self-calibration of laser scanners can be adopted for modeling the systematic errors if they cannot be eliminated/reduced through the observation procedure. The distinct points derived from the intersection of three planes can be used to replace signalized targets in the point-based deformation analysis. This newly proposed method is a simple extension to the point-based deformation analysis technique and it allows rotational movements of planes to be detected and measured. Simulation and real data show that this new method can measure translations better than a millimetre and rotations in the arc minute level when indoors. The main focus of future work will be to apply this method to larger indoor structures, such as the Olympic Oval in Calgary, Canada.

ACKNOWLEDGEMENTS

Research funding provided by the Natural Sciences and Engineering Research Council of Canada, Alberta Innovates, and Informatics Circle of Research Excellence, Terramatics Technologies Inc., and SarPoint Engineering Ltd. is gratefully acknowledged. The authors would also like to thank Kathleen Ang for proof-reading and editing this paper.

REFERENCES

- Alba, M., & Scaioni, M. (2010). Automatic detection of changes and deformation in rock faces by terrestrial laser scanning. *Proceedings of the ISPRS Commission V Mid-Term Symposium on Close Range Image Measurement Techniques*, vol. XXXVIII.
- Belton, D., & Lichti, D. (2006). Classification and segmentation of terrestrial laser scanner point clouds using local variance information. *The International Archives of the photogrammetry, Remote Sensing, and Spatial Information Sciences*, Vol. XXXVI, Part 5 , 44-49.
- Chow, J., Ebeling, A., & Teskey, W. (2010a). Low Cost Artificial Planar Target Measurement Techniques for Terrestrial Laser Scanning. *FIG Congress 2010: Facing the Challenges - Building the Capacity*. Sydney, Australia, April 11-16.
- Chow, J., Teskey, W., & Lichti, D. (2010b). Self-calibration and evaluation of the Trimble GX terrestrial laser scanner. *The International Archives of the Photogrammetry, Remote Sensing and Spatial Information Sciences 38 (Part 1)*.
- Gielsdorf, F., Gruendig, L., & Milev, I. (2008). Deformation analysis with 3D laser scanning. *Measuring the Changes - 13th FIG Symposium on Deformation Measurement and Analysis & 4th IAG Symposium on Geodesy for Geotechnical and Structural Engineering (In CD-ROM)*. Lisbon, Portugal. May 12-15.
- Gordon, S., & Lichti, D. (2007). Modeling terrestrial laser scanner data for precise structural deformation measurement. *Journal of Surveying Engineering 133(2)*, 72-80.
- Gründig, L., Neureither, M., & Bahndorf, J. (1985). Detection and localization of geometrical movements. *Journal of Surveying Engineering 111* , 118–132.
- Horn, B. (1987). Closed-form solution of absolute orientation using unit quaternions. *J. Opt. Soc. Amer. A*, 4(4) , 629-642.
- Lichti, D. (2007). Modelling, calibration and analysis of an AM-CW terrestrial laser scanner. *ISPRS Journal of Photogrammetry and Remote Sensing 61 (5)* , 307-324.

Lindenbergh, R., & Pfeifer, N. (2005). A statistical deformation analysis of two epochs of terrestrial laser data of a lock. In *Proceedings of Optical 3D Measurement Techniques, Vol II*, (s. 61-70). Vienna, Austria.

Monserrat, O., & Crosetto, M. (2008). Deformation measurement using terrestrial laser scanning data and least squares 3D surface matching. *ISPRS Journal of Photogrammetry and Remote Sensing* 63(1), 142-154.

Rönholm, P., Nuikka, M., Suomine, A., Salo, P., Hyypä, H., Pontinen, P., et al. (2009). Comparison of measurement techniques and static theory applied to concrete beam deformation. *Photogrammetric Record* 24(128), 351–371.

Shakarji, C. (1998). Least-squares fitting algorithms of the NIST algorithm testing system. *Journal of Research of the National Institute of Standards and Technology* 103 (6) , 633-641.

Soudarissanane, S., Lindenbergh, R., Menenti, M., & Teunissen, P. (2011). Scanning geometry: Influencing factor on the quality of terrestrial laser scanning points. *ISPRS Journal of Photogrammetry and Remote Sensing*, 66(4) , 389-399.

Vosselman, G., Gorte, B., Sithole, G., & Rabbani, T. (2004). Recognising structure in laser scanner point clouds. *International Archives of Photogrammetry, Remote Sensing and Spatial Information Sciences* 46(8/W2) , 33-38.

BIOGRAPHICAL NOTES

Jacky is currently a PhD student studying in the Geomatics Engineering department at the University of Calgary. He specializes in close-range digital imaging techniques for accurate 3D object space reconstruction and deformation monitoring. His research interests include: imaging sensor error modelling (e.g. self-calibration of terrestrial laser scanners, digital medium format cameras, and 3D range cameras), point cloud manipulation and processing (e.g. geometric form fitting, feature extraction, and classification), markerless point cloud registration techniques (e.g. ICP), multi-sensor integration, and deformation analysis.

Dr. William (Bill) Teskey is a Professor in the Department of Geomatics Engineering at the University of Calgary. He is a registered Professional Engineer in Alberta and a registered Land Surveyor in Alberta and Canada. Bill served for a number of years on the Western Canadian Board of Examiners for Land Surveyors and on the Board of Examiners of the Association of Professional Engineers, Geologists and Geophysicists of Alberta. His areas of interest are precise engineering and deformation surveys.

Bill Lovse is the Principal of Terramatic Technologies, Inc., Calgary, Alberta. Terramatic Technologies is an Industrial Partner in the "Low-Cost High-Precision Indoor/Outdoor 3D Laser Scanning" NSERC Collaborative Research and Development Project in which Jacky Chow is the Senior PhD Student and Bill Teskey is the Principal Investigator.

CONTACTS

Jacky C.K. Chow
Department of Geomatics Engineering
Schulich School of Engineering, University of Calgary
2500 University Drive N.W.
Calgary, Alberta, T2N 1N4
Canada
Tel. +1 (403) 220-3582
Fax + 1 (403) 284-1980
Email: jckchow@ucalgary.ca

Prof. Dr. William F. Teskey
Department of Geomatics Engineering
Schulich School of Engineering, University of Calgary
2500 University Drive N.W.
Calgary, Alberta, T2N 1N4
Canada
Tel. +1 (403) 220-7397
Fax + 1 (403) 284-1980
Email: wteskey@ucalgary.ca

J.W. (Bill) LOVSE
Terramatic Technologies Inc
Suite 12, 5080 12a St SE
Calgary, Alberta, T2G 5K9
Tel. +1 (403) 214-3655
Fax +1 (403) 214-1428
Email: bill@terramatic.com